Supporting information

Dual-responsive luminescent sensors based on two Cd-MOFs: rare enhancement toward acac and quenching toward $Cr_2O_7^{2-}$

Yu'e Yu [a], *Yuhao Wang* [a], *Haijun Xu* [b], *Jing Lu* [a], *Huaiwei Wang* [a], *Dacheng Li* [a], *Jianmin Dou* [a], *Yunwu Li* [a,*], *Suna Wang* [a,*]

[a] Shandong Provincial Key Laboratory of Chemical Energy Storage and Novel Cell Technology, School of Chemistry and Chemical Engineering, Liaocheng University, Liaocheng, 252059, P. R. China.

[b] Jiangsu Co-Innovation Center of Efficient Processing and Utilization of Forest Resources, College of Chemical Engineering, Nanjing Forestry University, Nanjing 210037, China.

Email: wangsuna@lcu.edu.cn, liyunwu@lcu.edu.cn

Content

Experimental details

Synthesis of the ligand.

The ligand H_3L was synthesized by adding Dimethyl 5-aminoisophthalate (2.09 g, 10 mmol) and methyl-4-formylbenzoate (1.64 g, 10 mmol) mixture in a 250 mL flask, then 100 mL of methanol was added, and 5 drops of glacial acetic acid were added as a reaction catalyst, refluxing and stirring were carried out for 12 h at 70 °C. After, the mixture was cooled, filtered and washed with methanol several times, a white solid (a) is obtained. The intermediate (a) (1.77 g, 5.0 mmol) was thoroughly dissolved in a mixture of 30 mL of dichloromethane and 20 mL of methanol, then $NaBH_4$ (0.23 g, 6.0 mmol) was added, and stirred at room temperature for 10 h. After a series of treatments, a white solid (b) is obtained. The intermediate (b) (0.535 g, 1.5 mmol) was completely dissolved in 50 mL THF, then NaOH aqueous solution (1.25 mol/L, 30 mmol) was added and the mixture was stirred and refluxed for 24 h at 60 °C. After the solution was concentrated under vacuum, diluted HCl solution (5 mol/L) was added until the pH value was less than 1 and stirred for 2 h. After filtered and washed with water, the light yellow solid of H_3L was obtained.

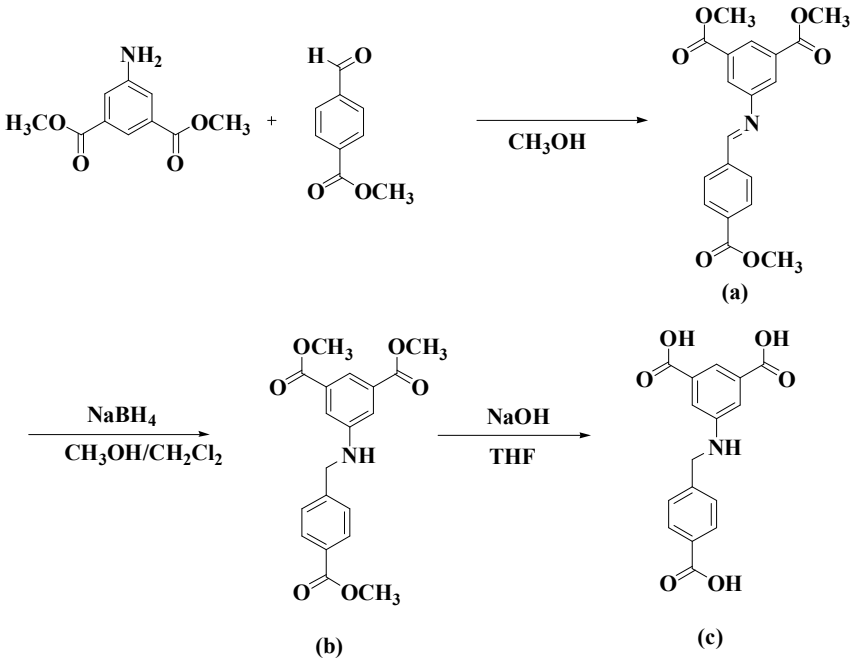

Scheme 1. Synthesis of H_3L.

Luminescent sensing experiments.

The luminescence titration experiments of **Cd-MOFs** toward acac were executed as below. Diverse amounts of acac solutions in DMF (10^{-3} M) were introduced to a quartz cuvette containing 4.0 mL of DMF suspension with 2 mg **LCU-107** or **LCU-108.** The PL spectra were then detected with the precise volume of the solutions. The interference experiments were performed as below: acac/$Cr_2O_7^{2-}$ (10^{-3} M, 2.0 mL) and other small organic molecules/anions (10^{-3} M, 2.0 mL) were introduced into the 2 mg samples of two MOFs to form suspensions (4.0 mL) containing equal acac/$Cr_2O_7^{2-}$ and other mall organic molecules/anions with a total concentration of 10^{-3} M.

In the recycling experiments, the MOF samples after first sensing were collected by centrifugation, washed thoroughly with DMF, and subsequently reused.

X-ray crystallographic study.

Single-crystal X-ray data for two Cd-MOFs were collected on a Siemens Smart CCD diffractometer with graphite-monochromatic Mo Kα radiation (λ = 0.71073 Å) at 298 K. The raw data frames were integrated into SHELX-format reflection files and corrected using SAINT program.[1] Absorption corrections based on multi-scan were obtained by the SADABS program.[2] The structure was solved with direct methods SHELXS[3] and refined with full-matrix least-squares technique using the SHELXL-2014/7 programs.[4] Displacement parameters were refined anisotropically, and the positions of the H-atoms were generated geometrically, assigned isotropic thermal parameters, and allowed to ride on their parent carbon atoms before the final cycle of refinement. There are some solvent accessible void volumes in **LCU-107**, which are occupied by highly disordered DMF and H_2O molecules. No satisfactory disorder model could be achieved, and therefore the SQUEEZE program implemented in PLATON was used to remove the electron densities.[5] The solvents are tentatively assigned based on TGA, elemental analysis as well as the SQUEEZE results. The structure was examined using the Addsym subroutine of PLATON to ensure that no additional symmetry could be applied to the models. Basic information pertaining to crystal parameters and structure refinement is summarized in Table S1 and selected bond lengths and angles are listed in Table S2.

Table S1. Crystal and refinement data for two Cd-MOFs.

	LCU-107	**LCU-108**
Empirical formula	$C_{30.5}H_{32}N_{4.5}O_{8.75}Cd$	$C_{31}H_{34}N_4O_9Cd$
Formula weight	714.02	719.02
Temperature/ K	298	298
Crystal system	monoclinic	triclinic
Space group	$P2_1/c$	P_{-1}
a [Å]	11.8718(9)	10.3690(9)
b [Å]	17.9778(15)	10.4966(9)
c [Å]	15.3222(13)	15.0556(13)
α [˚]	90	101.026(2)
β [˚]	96.405(2)	95.922(1)
γ [˚]	90	96.615(1)
Volume/A^3	3249.8(5)	1584.5(2)
Z	4	2
D(calc)[g/cm^{-3}]	1.189	1.507
μ [mm^{-1}]	0.707	0.748
θ range	2.3-25	2.6-25.0
Index ranges	-14<=h<=13, -21<=k<=21, -18<=l<=18	-12<=h<=12, -12<=k<=10, -15<=l<=17
aR1;bwR2 [I> 2σ(I)]	0.1336, 0.3413	0.0523, 0.1452
GOF	1.54	0.98

Table S2. Selected bond lengths [Å] and angles [º] for two Cd-MOFs**.**

LCU-107			
Cd(1)-O(1)	2.415(11)	Cd(1)-O(2)	2.486(12)
Cd(1)-N(2)	2.281(12)	Cd(1)-N(3C)	2.423(12)
Cd(1)-O(3A)	2.388(11)	Cd(1)-O(4A)	2.590(11)
Cd(1)-O(4B)	2.397(11)	O(1)-Cd(1) -O(2)	91.5(4)
O(1)-Cd(1)-N(2)	91.1(4)	O(1)-Cd(1)-N(3C)	92.1(5)
O(1)-Cd(1)-O(3A)	82.2(4)	O(1)-Cd(1)-O(4A)	135.2(4)
O(1)-Cd(1)-O(4B)	149.7(4)	O(2)-Cd(1)-N(2)	87.5(4)
O(2)-Cd(1)-N(3C)	92.8(4)	O(2)-Cd(1)-O(3A)	136.2(4)
O(2)-Cd(1)-O(4A)	170.3(4)	O(2)-Cd(1)-O(4B)	95.6(4)
N(2)-Cd(1) -N(3C)	177.0(4)	O(3A)-Cd(1)-N(2)	90.6(4)
O(4A)-Cd(1)-N(2)	89.4(4)	O(4B)-Cd(1 -N(2)	87.6(4)
O(3A)-Cd(1)-N(3C)	91.3(4)	O(4A)-Cd(1)-N(3C)	89.8(4)
O(4B)-Cd(1)-N(3C)	89.4(4)	O(3A)-Cd(1)-O(4A)	53.0(3)
O(3A)-Cd(1)-O(4B)	128.1(4)	O(4A)-Cd(1)-O(4B)	75.1(4)

Symmetry codes: A. 1-x, 0.5+y, 1.5-z. B. x, 1.5-y,0.5+z C. -1+x, y, z.

LCU-108			
Cd(1)-O(1)	2.371(3)	Cd(1)-O(7)	2.379(4)
Cd(1)-O(2)	2.414(3)	Cd(1)-N(2)	2.440(4)
Cd(1)-N(3B)	2.352(4)	Cd(1)-O(4A)	2.224(3)
O(1)-Cd(1)-O(2)	55.09(11)	O(1)-Cd(1)-O(7)	88.02(13)
O(1)-Cd(1)-N(2)	88.16(12)	O(1)-Cd(1)-C(1)	27.50(13)
O(1)-Cd(1)-N(3B)	143.58(13)	O(1)-Cd(1)-O(4A)	89.72(12)
O(2)-Cd(1)-O(7)	90.59(12)	O(2)-Cd(1)-N(2)	86.68(12)
O(2)-Cd(1)-C(1)	27.59(13)	O(2) -Cd(1)-N(3B)	88.55(13)
O(2) -Cd(1)-O(4A)	144.80(12)	O(7)-Cd(1)-N(2)	176.12(14)
O(7)-Cd(1)-C(1)	88.98(14)	O(2)-Cd(1)-O(4A)	144.80(12)
O(7)-Cd(1)-N(2)	176.12(14)	O(7)-Cd(1)-C(1)	88.98(14)
O(7)-Cd(1)-N(3B)	90.54(15)	O(4B)-Cd(1)-O(7)	87.10(14)
N(2)-Cd1-C(1)	87.32(14)		

Symmetry codes: A: 1+x, y, z.; B: x, 1+y, z.

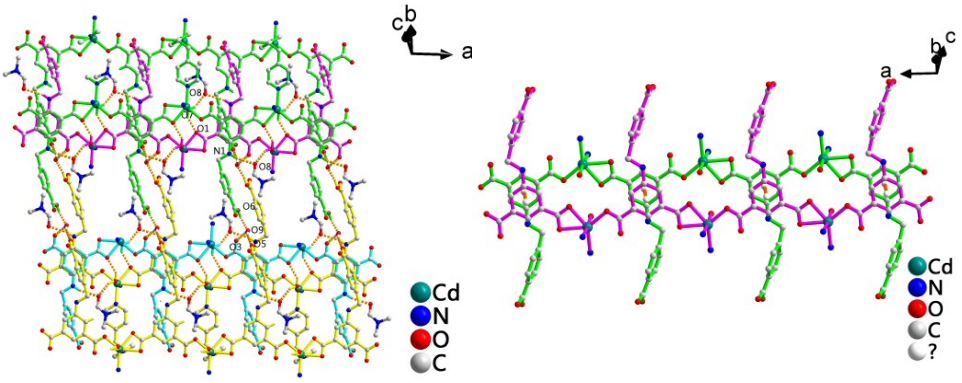

(a) (b)

Fig. S1. (a) Hydrogen bonding between layers of **LCU-108.** (b) The weak π···π stacking interactions between neighboring aromatic rings in **LCU-108**.

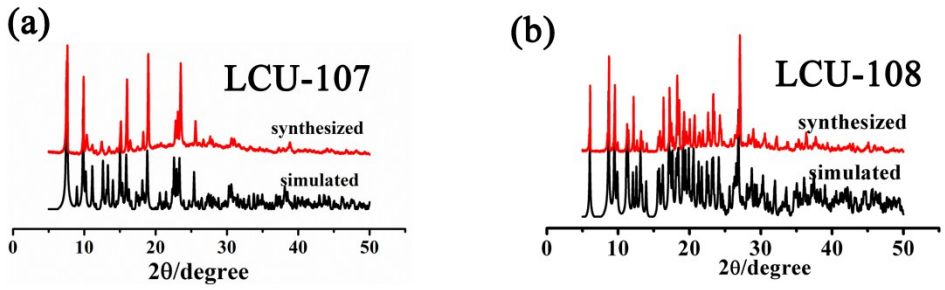

Fig. S2. PXRD of two Cd-MOFs.

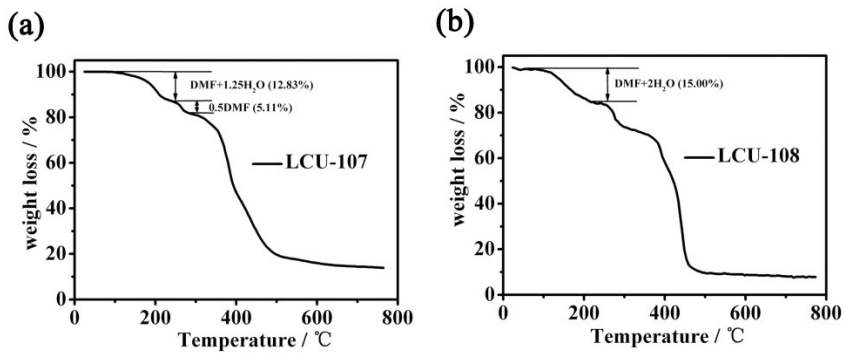

Fig. S3. TG of two Cd-MOFs.

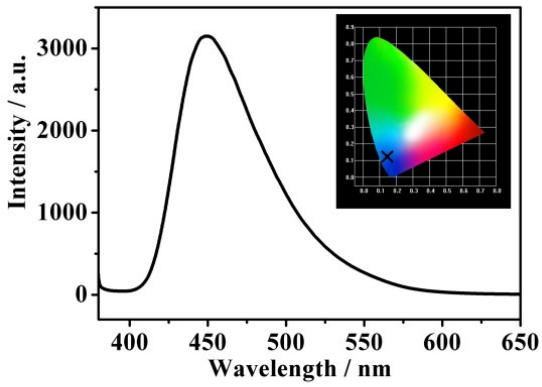

Fig. S4. The emission spectra and CIE coordinates of H_3L in the solid state.

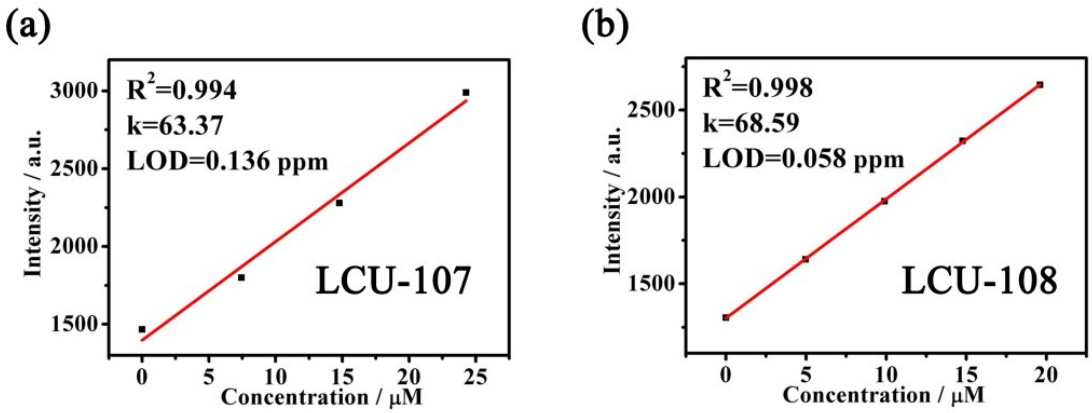

Fig. S5. LOD calculation of two Cd-MOFs toward acac in DMF.

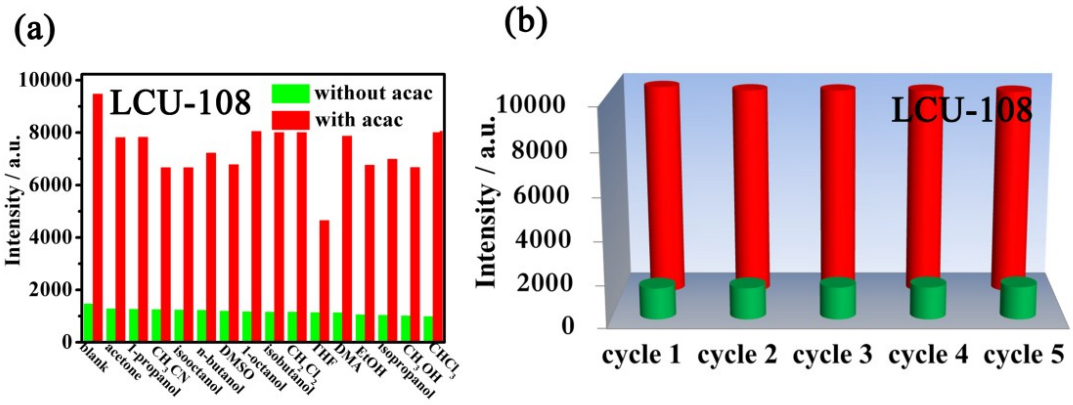

Fig. S6. (a) Interference experiment results of **LCU-108** in the suspensions of different organic molecules with and without acac, respectively. (b) The recycling luminescence intensity of **LCU-108** after five runs. The intensities before and after acac introduced were represented by green and red bars, respectively.

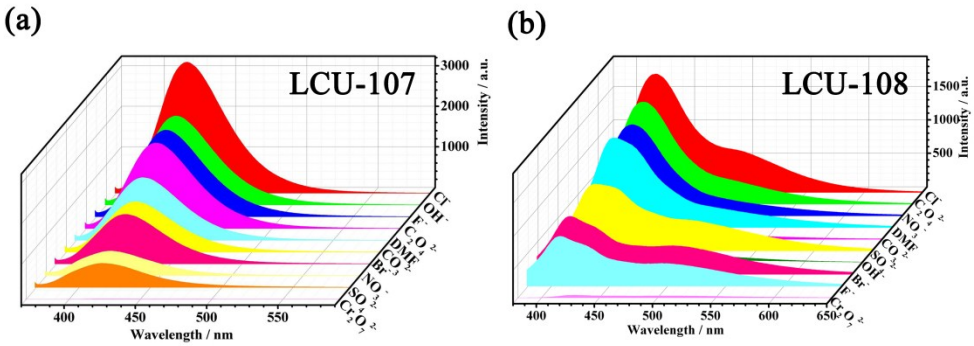

Fig. S7. (a) and (b) Luminescence spectra of two Cd-MOFs in DMF with different anions (10^{-3} M).

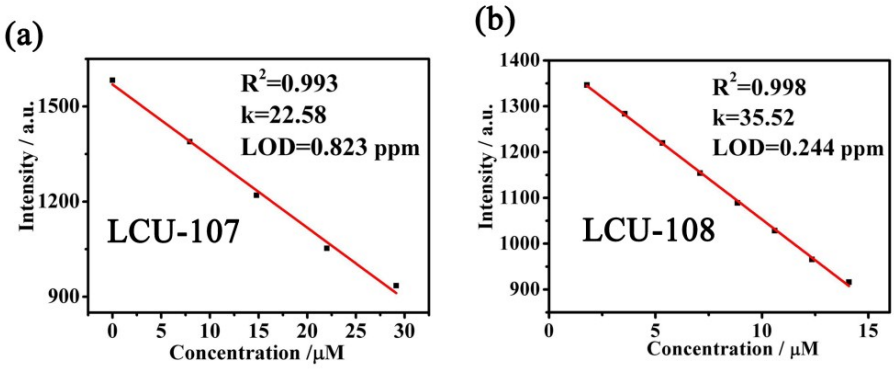

Fig. S8. LOD calculation of two Cd-MOFs toward $Cr_2O_7^{2-}$ in DMF.

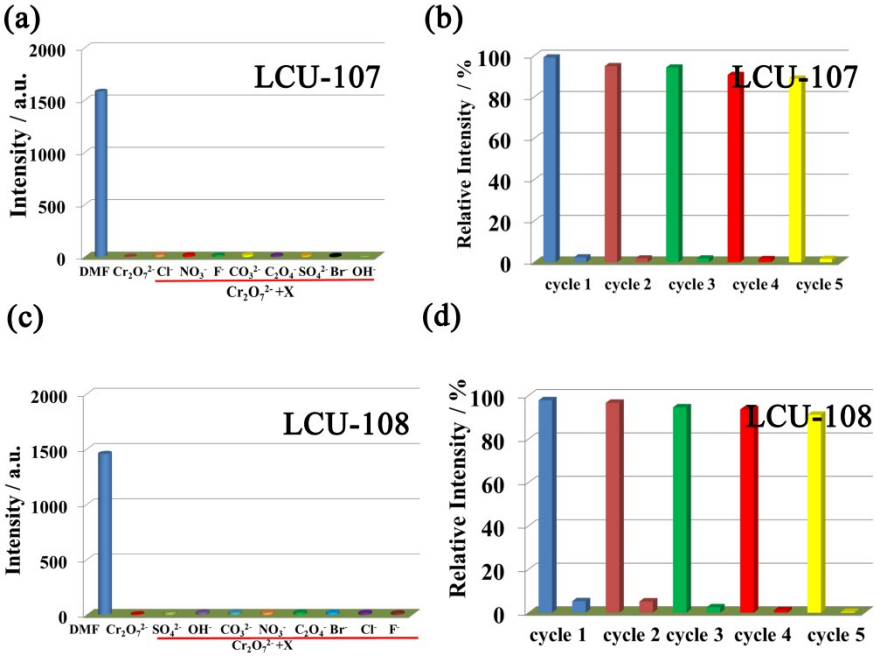

Fig. S9. (a) and (c) Luminescence intensities of two Cd-MOFs with the addition of $Cr_2O_7^{2-}$ ions with the existence of other anions in DMF. (b) and (d) The relative luminescence intensities of two Cd-MOFs toward $Cr_2O_7^{2-}$ in the recycling experiments.

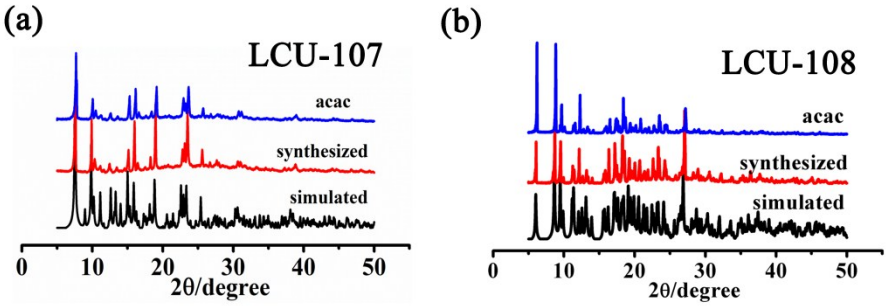

Fig. S10. PXRD of two Cd-MOFs soaked in DMF containing acac for three days.

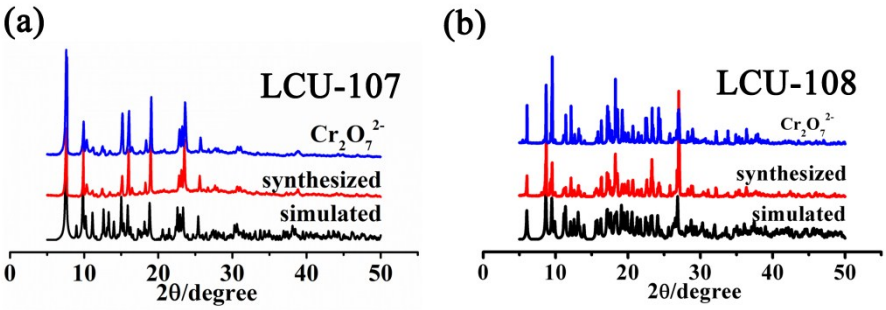

Fig. S11. PXRD of two Cd-MOFs soaked in DMF containing $Cr_2O_7^{2-}$ for three days.

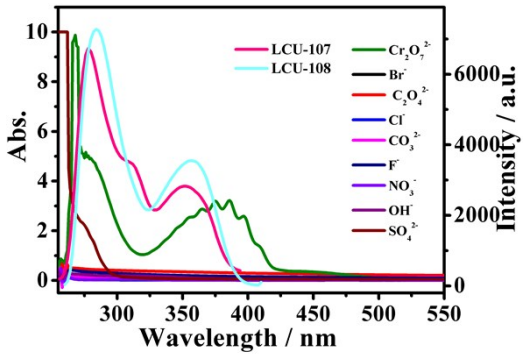

Fig. S12. UV–Vis spectra of different anions in DMF and excitation spectra of two Cd-MOFs.

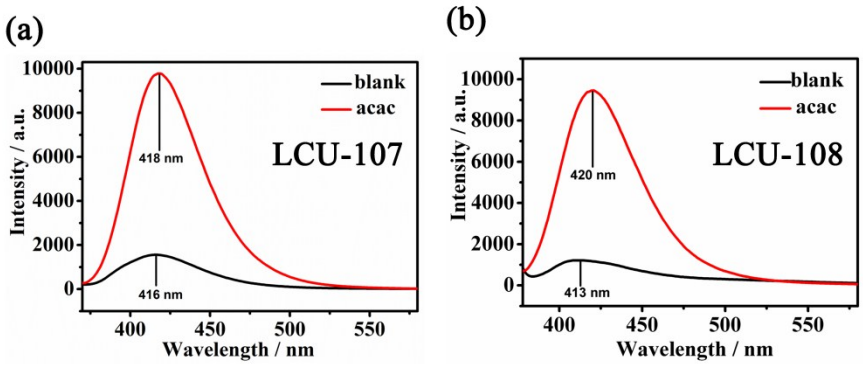

Fig. S13. Luminescence spectra of two Cd-MOFs in DMF with acac.

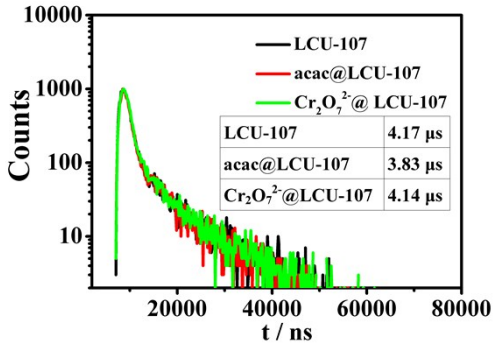

Fig. S14. The luminescence decay lifetimes of the original **LCU-107** and acac, $Cr_2O_7^{2-}$ treated **LCU-107**.

Table S3. Performance comparison between various MOFs/CPs fluorescent sensors.

acac				
MOFs/CPs	detection process	K_{SV}/M^{-1}	LOD	Refs.
$\{[Zn(XL)_2](ClO_4)_2\cdot 6H_2O\}_n$	turn-off	7.382×10^3	1.72 ppm	[6]
$\{[(CH_3)_2NH_2][Zn(FDA)(BTZ)_2]\}_n$	turn-off	1.86×10^5	0.647μM	[7]
$\{[Zn_2(XN)_2(IPA)_2]\cdot 2H_2O\}_n$	turn-off	2.3×10^3	0.25 ppm	[8]
$\{[Cd(L)(1,4\text{-}PDA)]\cdot 0.7(C_2H_5OH)\}_n$	turn-off	4.09×10^3	2.45μM	[9]
$\{[Cd(L)_{0.5}(1,8\text{-}NDC)\cdot H_2O]\}_n$	turn-off	7.75×10^3	1.40μM	[9]
$\{[Eu(bcpt)(HCOO)]\cdot 0.5H_2O\}_n$	turn-off	322	1.21×10^{-4}M	[10]
$[Cd(L)(NTA)]_n$	turn-off	1258	3.63μM	[11]
$\{[Zn_3(bbib)_2(ndc)_3]\cdot 2DMF\cdot 2H_2O\}_n$	turn-on	-	0.10 ppm	[12]
$\{[Cd(HL1)(bpy)]\cdot 3H_2O\cdot DMF\}_n$	turn-on	2.11×10^4	0.136 ppm	this work
$\{[Cd(HL1)(bpea)\cdot H_2O]\cdot H_2O\cdot DMF\}_n$	turn-on	2.14×10^4	0.058 ppm	
$Cr_2O_7^{2-}$				
MOFs/CPs	detection process	K_{SV}/M^{-1}	LOD	Refs.
[Zn(IPA)(L)]n	turn-off	1.37×10^3	12.02μM	[13]
$[Eu(HL)(H_2O)_2(NO_3)]\cdot NO_3$	turn-off	7.52×10^4	1.7×10^{-5}M	[14]
$[Tb(HL)(H_2O)_2(NO_3)]\cdot NO_3$	turn-off	4.99×10^4	2.5×10^{-5}M	[14]
$[Tb(ppda)(bdc)_{0.5}(C_2H_5OH)(H_2O)]_n$	turn-off	4.03×10^3	5.0×10^{-5}M	[15]
$\{[Cd(L1)(BPDC)]\cdot 2H_2O\}_n$	turn-off	6.40×10^3	37.60μM	[16]
$\{[Cd(L1)(SDBA)(H_2O)]\cdot 0.5H_2O\}_n$	turn-off	4.97×10^3	48.60μM	[16]
$\{[Cd(HL)(bpy)]\cdot 3H_2O\cdot DMF\}_n$	turn-off	2.42×10^4	0.823 ppm	this work
$\{[Cd(HL)(bpea)\cdot H_2O]\cdot H_2O\cdot DMF\}_n$	turn-off	3.86×10^4	0.244 ppm	

XL=N,N'-bicyclo[2.2.2]oct-7-ene-2,3,5,6-tetracarboxdiimide bi(1,2,4-triazole)[6]

H_2FDA = furan-2,5-dicarboxylic acid[7]

HBTZ = 1H-benzotriazole[7]

XN=4'-(4-pyridine)4,2':2',4''-terpyridine[8]

IPA= isophthalic acid[8]

L=1,4-bis(5,6-dimethybenzimidazol-1-yl)-2-butene[9]

1,4-H_2PDA = 1.4-phenylenediaceticacid[9]

1,8-H_2NDC = 1,8-naphthalenedicarboxylic acid[9]

L1=1,4-bis(benzimidazol-1-yl)-2-butylene[10]

1,4-H_2NDC = 1,4-naphthalenedicarboxylic acid[10]

L = 1,6-bis(benzimi-dazol-1-yl)hexane[11]

H_2NTA = 2-nitroterephthalic acid[11]

bbib=1,3-bis(benzimidazolyl)benzene[12]

H_2ndc=1,4-naphthalenedicarboxylic acid[12]

L = 3-pyridylcarboxaldehydenicotinoylhydrazone[13]

H_2IPA = isophthalic acid[13]

H_2L =4-(3,5-dicarboxyl-phenyl)-2-methylpyridine[14]

H_2ppda =4-(pyridin-3-yloxy)-phthalic acid[15]

H_2bdc =terephthalic acid[15]

L1 = 4,4'-(2,5-bis-(methylthio)-1,4-phenylene)dipyridine[16]

H_2BPDC = 4,4'-biphenyldicarboxylic acid[16]

H_2SDBA = 4,4'-sulfonyldibenzoic acid[16]

References:

1 SAINT, Version 6.02a; Bruker AXS Inc, Madison, WI, 2002.

2 G. M. Sheldrick, SADABS, Program for Brucker Area Detector Absorption Correction; Göttingen University: Göttingen, Germany, 1997.

3 G. M. Sheldrick, A short history of SHELX. *Acta Crystallogr. Sec. A: Found. Crystallogr.* 2008, **64**, 112−122.

4 G. M. Sheldrick, Crystal structure refinement with SHELXL. *Acta Crystallogr. Sec. C: Struct. Chem.* 2015, **71**, 3−8.

5 A. L. Spek, *J. Appl. Cryst.* 2003, **36**, 7.

6 X. M. Kang, R. R. Cheng, H. Xu, W. M. Wang and B. Zhao, *Chem. Eur. J.*, 2017, **23**, 13289–13293.

7 J. Y. Zou, L. Li, S. Y. You, K. H. Chen, X. N. Dong, Y. H. Chen and J. Z. Cui, *Cryst. Growth. Des.*, 2018,**18**, 3997−4003.

8 X. M. Kang, X. Y. Fan, P. Y. Hao, W. M. Wang and B. Zhao., *Inorg. Chem. Front.*, 2019, **6**, 271–277.

9 Y. S. Shi, Y. H. Li, G. H. Cui and G.Y. Dong, *CrystEngComm.*, 2020, **22**, 905–914.

10 Y. J. Yang, Y. H. Li, D. L. Liu and G. H. Cui, *CrystEngComm.*, 2020, **22**, 1166–1175.

11 H. Zhu, C. Han, Y. H. Li and G. H. Cui, *J. Solid State Chem.* 2020, **282**, 121132-121139.

12 S. L. Yao, S. J. Liu, X. M. Tian, T. F. Zheng, C. Cao, C. Y. Niu, Y. Q. Chen, J. L.

Chen, H. P. Huang and H. R. Wen, *Inorg. Chem*., 2019, **58**, 3578−3581.

13 B. Parmar, Y. Rachuri, K. K. Bisht, R. Laiya and E. Suresh, *Inorg. Chem*., 2017, **56**, 2627-2638.

14 W. Gao, F. Liu, B. Y. Zhang, X. M. Zhang, J. P. Liu, Q. Gao and Q. Y. Gao, *Dalton Trans*., 2017, **46**, 13878-13887.

15 X. L. Zhang, Z. Y. Zhan, X. Y. Liang, C. Chen, X. L. Liu, Y. J. Jia and M. Hu, *Dalton Trans*., 2018, **47**, 3272-3282.

16 S. G. Chen, Z. Z. Shi, L. Qin, H. L. Jia and H. G. Zheng, *Cryst. Growth Des*. 2017, **17**, 67-72.